Cell cycle diversity involves differential regulation of Cyclin E activity in the *Drosophila* bristle cell lineage

Agnès Audibert, Françoise Simon and Michel Gho*

UMR 7622, CNRS-University Paris VI. 9, Quai Saint Bernard, 75005 Paris, France
*Author for correspondence (e-mail: michel.gho@snv.jussieu.fr)

Summary

In the *Drosophila* bristle lineage, five differentiated cells arise from a precursor cell after a rapid sequence of asymmetric cell divisions (one every 2 hours). We show that, in mitotic cells, this rapid cadence of cell divisions is associated with cell cycles essentially devoid of the G1-phase. This feature is due to the expression of Cyclin E that precedes each cell division, and the differential expression of the S-transition negative regulator, Dacapo. Thus, apart from endocycles (G/S), which occurred in two out of five terminal cells, two other cell cycles coexist in this lineage: (1) an atypical cell cycle (S/G2/M), in which the S-phase is initiated during the preceding telophase; and (2) a canonical cell cycle (G1/S/G2/M) with a brief G1 phase. These two types of cell cycle result from either the absence or very transient expression of Dap, respectively. Finally, we show that the fate determinant factor, Tramtrack, downregulates Cyclin E expression and is probably involved in the exit of the cells from the cell cycle.

Key words: BrdU, Dacapo, G1-phase, In vivo, Microchaete, Tramtrack, *Drosophila*

Introduction

In several well-studied systems, organ development depends on the execution of a stereotyped pattern of cell divisions that constitute invariant cell lineages. Thus, in these lineages, the control of the cell cycle is essential for organ integrity and diverse types of cell cycles can be observed. Among these cell cycles, the canonical type is characterised by the alternation of a DNA replication phase (S-phase) and mitosis (M-phase) separated by two Gap-phases (G1 between M and S and G2 between S and M). Cell cycles that differ from this canonical G1/S/G2/M cycle have also been described (Vidwans and Su, 2001). For example, in a wide variety of cell types, the cell cycle consists of repeated rounds of S-phases without intervening mitoses. These endocycles generate polyploid cells that are frequently associated with large-scale transcription activity (Edgar and Orr-Weaver, 2001).

Control of cell cycle progression depends on an evolutionary conserved mechanism that regulates the transition between cell-cycle phases. For example, G1 cyclins associate with the cyclin-dependent kinase Cdk2 (Cdc2c – FlyBase) to promote initiation and progression through the S-phase. Differential regulation of these Cdk/Cyc complexes gives rise to the different types of cell cycle. In *Drosophila*, as in mammals, recent studies have shown that CycD/Cdk4 acts primarily as a cell growth regulator (Malumbres et al., 2004; Meyer et al., 2002a). By contrast, Cyclin E (CycE) appears to be the most important cyclin for the G1 to S transition (Knoblich et al., 1994; Richardson et al., 1995). Thus, maternal CycE is prevalent during the first embryonic cell cycles that lack a G1-phase. After degradation of the maternal stock of CycE, zygotic transcription of the *cycE* gene begins and cells transcribing *cycE* continue to proliferate, while those that do not express CycE stop proliferating. The correlation between CycE expression and cell proliferation suggests that progression to a postmitotic state depends on the downregulation of CycE (Richardson et al., 1995).

Dacapo (Dap), a protein related to the p21/p27 cyclin-dependent kinase inhibitor (CKI) family, plays an essential role in the downregulation of CycE (de Nooij et al., 1996; Lane et al., 1996). In *Drosophila dap* mutant embryos, most cells in the epidermis and in the peripheral nervous system fail to exit from the mitotic cell cycle at the appropriate time, and subsequently undergo an additional mitotic division (Meyer et al., 2002b).

The *Drosophila* cell lineage that generates mechanosensory bristles has been used as a model system to study cell determination, asymmetric cell divisions and cell polarity (Jan and Jan, 1998). In the notum, each bristle is composed of four cells: two outer cells (the socket and the shaft cells) and two inner cells (the neuron and the sheath cell). These cells originate from a unique precursor cell, pI, after four rounds of asymmetric divisions that occur during the pupal stages of development. pI cells are specified in a regular pattern of rows in the dorsocentral region of the notum around 6-9 hours after pupal formation (APF) (Usui and Kimura, 1993) and begin to divide around 16-17 hours APF to generate two secondary precursor cells, pIIa and pIIb. Later, pIIb divides before pIIa giving rise to a glial cell and a tertiary precursor cell, pIIIb. The division of pIIa generates a socket and a shaft cell. Next, the pIIIb cell divides to produce a neuron and a sheath cell (Gho et al., 1999). Finally, the glial cell undergoes apoptosis (Fichelson and Gho, 2003). Thus, only four cells of the bristle

lineage ultimately form each sensory organ. Upon completion of the lineage, cells enter a postmitotic stage in which the expression of specific factors controls their differentiation. For example, the Tramtrack (Ttk) transcription factor is expressed in all cells except the neuron. Its loss of function transforms sheath cells into neurons, while its overexpression produces the opposite effect (Guo et al., 1995).

We have used the *Drosophila* mechanosensory bristle as a model system to study cell cycle progression in a fixed cell lineage. Previous studies have shown that sensory mother cells are selected during the G2-phase and arrested in this phase until they resume mitosis and initiate the lineage (Kimura et al., 1997). Using a real-time approach at the single cell level, we describe the timing of cell cycle phases and their regulation in each cell of the bristle lineage. Our data show that three types of cell cycles are present: the canonical cell cycle (G1/S/G2/M), a cycle without the G1-phase (S/G2/M) and the endocycle (S/G). The two former mitotic cell cycles in this lineage depend on the differential expression of CycE and Dap. In addition, we present evidence that Ttk, which controls non-neural cell identity acquisition, downregulates CycE expression and probably participates in the exit of the cell from the cell cycle and its entrance into a postmitotic state. We propose that atypical cell cycles, together with asymmetric cell divisions, assure the rapid cadence of cell divisions observed in this lineage.

Materials and methods

Fly strains

The GAL4/UAS expression system (Brand and Perrimon, 1993) was used to express the following constructions in the mechanosensory bristle cell lineage: UAS-histone H2B::YFP (H2B::YFP) (Bellaiche et al., 2001), UAS-CyclinE (UAS-CycE) (Lane et al., 1996; Richardson et al., 1995), UAS-Dacapo (UAS-Dap) (Lane et al., 1996), UAS-Tramtrack69 (UAS-Ttk) (Badenhorst, 2001). As GAL4-drivers, we used the lines neuralized[p72]-Gal4 (Bellaiche et al., 2001) and hs-Gal4 (gift from A. Brand), which drives GAL4 in all cells after heatshock. CycE overexpressions were carried out using a line harbouring two copies of the UAS-CycE construct, one on the second and one on the third chromosome, respectively. The dap^4 is a null allele of *dap* (Hong et al., 2003). The A101 lines carry a P(LacZ, ry+) enhancer trap of *neuralized* and specifically expresses nuclear β-gal in pI and its progeny cells (Usui and Kimura, 1993).

Combining time-lapse in-vivo imaging and BrdU incorporation

In-vivo imaging was carried out as described previously on neu^{p72}> H2B::YFP pupae (Gho et al., 1999). Imaging was acquired every 4 minutes on an Olympus BX-41 fluorescence microscope (20× or 40× objective) equipped with a CoolSnap camera driven by Metaview software (Universal Imaging). The temperature was 25°C. Time-lapse movies were assembled using NIH image software. Sensory clusters were identified according to their relative positions on the thorax. For each identified cluster, time from the previous metaphase was recorded to determine the age of the cells.

At a given time, the notum from the imaged pupae was dissected and incubated with 50 μg/ml BrdU in M3 culture medium complemented with fetal bovine serum (2%), insulin (0.1 U/ml) and ecdyson (0.5 μg/ml), for 10 or 15 minutes at 25°C. Immediately after, the notum was fixed for 20 minutes in 4% paraformaldehyde. To detect bristle lineage cells and/or specific proteins, immunoreaction was realized as described below. The notum was refixed in 4% paraformaldehyde for 15 minutes. To detect incorporated BrdU, the notum was treated twice in 2N HCl for 15 minutes each and subsequently neutralized in 0.1 mol/l $Na_2B_4O_7$ for 5 minutes. BrdU was detected using mouse monoclonal anti-BrdU (Becton Dickinson 1:50), and Alexa 488- and 568-conjugated secondary antibodies (Molecular Probes, 1:1000). Time of each cell was calculated as the time determined from the in-vivo imaging plus 15 minutes, the period corresponding to the dissection and BrdU incubation. The BrdU index was calculated as the percentage of the number of BrdU-positive clusters relative to the total number of clusters analysed.

To analyse the pattern of CycE expression, in-vivo recordings were obtained as before, but the notum was dissected, immediately fixed and the immunoreaction was performed.

Immunohistology

Dissected nota from pupae at 15-35 hours APF were processed as described in Gho et al. (Gho et al., 1996). The following primary antibodies were used: rat anti-α-tubulin (Serotec, 1:500), rabbit anti-β-gal (Cappel, 1:500), mouse anti-β-gal (Promega, 1:1000); mouse anti-Cut (DSHB, 1:500), guinea pig anti-Sens (1:1000) (Nolo et al., 2000), rabbit anti-GFP (Santa-Cruz, 1:500), mouse anti-GFP (Roche, 1:500), rat anti-CycE (gift from H. Richardson, 1:1000), mouse anti-Dap (gift from H. Hariharan, 1:4), rabbit anti-Dap (gift from C. Lehner, 1:300), rabbit anti-Lamin (gift from P. Fisher, 1:4000), rat anti-Ttk (gift from F. Schweisguth, 1:300), rat anti-ELAV (DSHB, 1:10), mouse anti-ELAV (DSHB, 1:100), rat anti-Su(H) (gift from F. Schweisguth, 1:500). Alexa 488- and 568-conjugated secondary antibodies anti-mouse, anti-rat, anti-rabbit and anti-guinea pig were purchased from Molecular Probes and used at 1:1000. Cy5 conjugated antibodies anti-mouse, -rat or -rabbit were provided from Promega and were used at 1:2000. Images were processed with NIH-Image and Photoshop software.

Clonal analysis and heatshock

Somatic clones were obtained using the FLP/FRT recombination system. The w; FRT^{82B} ttk^{1e11} line (Baonza et al., 2002) was crossed to the hs-flp, FRT^{82B} ubq-nls::GFP (gift from J.-R. Huynh) to generate ttk^{1e11} somatic clones. To induce mitotic recombination, second instar larvae were heatshocked twice at 38°C for 30 minutes at 1 hour intervals and kept at 25°C for recovery. Heatshocked overexpression was realized using the hs-Gal4>Ttk69 line. Pupae were collected at puparium formation and aged to determined time. Heatshock was performed at 38°C for 30 minutes and pupae were kept for 4 hours at 25°C for recovery.

Results

Characterisation of cell cycle phases in the bristle lineage

To determine the chronology of the different cell cycle phases in the bristle lineage, we analysed cells that entered into and exited from S- and M-phases. From these observations, we deduced the timing and the duration of the interposed G1- and G2-phases. Mitosis in the bristle lineage was analysed in vivo with a Histone2B::YFP (H2B::YFP) fusion protein (Bellaiche et al., 2001) expressed in the bristle lineage cells using the Gal4/UAS expression system (Brand and Perrimon, 1993). YFP-fusion protein was driven by the neu^{p72} fly line that harbours a pGAL4 insertion on the *neuralized* gene promoter (Bellaiche et al., 2001). The S-phase was monitored using an original experimental protocol, which combined time-lapse imaging in a live pupa and subsequent BrdU incorporation in tissue culture. Time-lapse imaging of neu^{p72}> H2B::YFP live pupa was used to follow the cell lineage of several precursor cells (Fig. 1A,D). This allowed us to determine the exact time
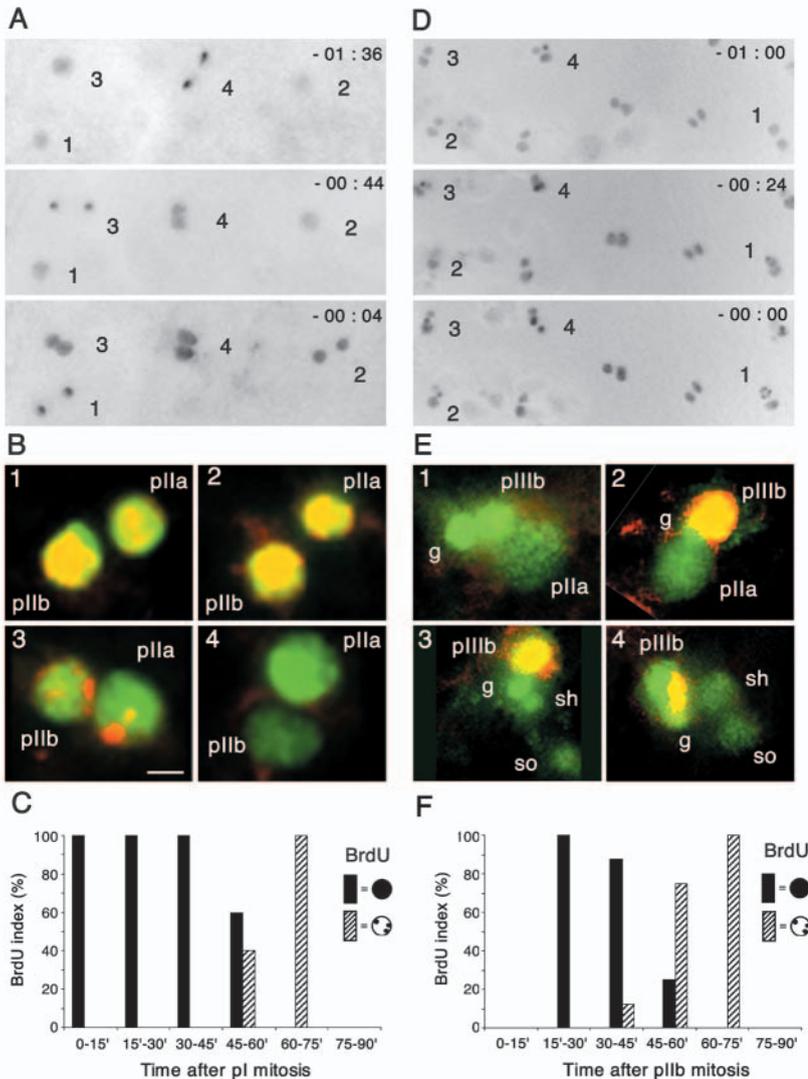
Fig. 1. Characterization of the S-phase in pIIa and pIIb precursor cells (A-C) and pIIIb precursor cells (D-F). A strategy combining time-lapse imaging (A,D) and BrdU incorporation (B,E) was used to define the duration of the S-phase in these cells. (A,D) Time-lapse analysis of living neu^{P72}> H2B::YFP pupae at 17 hours APF (A) and 19 hours APF (D). Time (h:min) before the end of the time-lapse recording is shown at the top of each frame. (B,E) BrdU incorporation in the same clusters as in A and D, respectively (numbered from 1 to 4). BrdU incorporation is revealed in red, and lineage cells were identified by specific anti-Sens immunoreactivity (green). In B, the time following the end of the corresponding pI metaphase, determined by time-lapse recording, was 19 minutes for cluster 1, 27 minutes for cluster 2, 59 minutes for cluster 3 and 1 hour 56 minutes for cluster 4. Note that both precursor cells exit the S-phase at the same time, as suggested by the punctuated BrdU labelling (B, cluster 3). In E, the time after the end of the corresponding pIIb metaphase was 7 minutes for cluster 1, 19 minutes for cluster 2, 39 minutes for cluster 3 and 1 hour 15 minutes for cluster 4. Note that BrdU incorporation was observed only in the pIIIb cell, recognized by the size of the nucleus and its anterior position in the cluster. (C,F) Histograms showing the percentage of BrdU-positive clusters as a function of time after pI (C) and pIIb (F) metaphase. Black bars correspond to cell pairs in which BrdU incorporation was homogeneous throughout the nuclei. Hatched bars correspond to cell pairs in which punctuated BrdU incorporation was observed. Note in F that no BrdU incorporation was observed before 15 minutes after pIIb division. In both histograms, bars were calculated after analysis of at least 5 clusters. Scale bar: 2 µm.

of mitosis entry for each cell. At given times, the notum was dissected and placed in a BrdU-containing culture medium for 10 minutes and then fixed. BrdU revelation showed the cells that are in the S-phase during the 10-minute incubation period (Fig. 1B,E). As each cell cluster was followed throughout the in-vivo recording session, we know their exact time of birth. Thus, it was possible to accurately determine the beginning and the end of the S-phase for each cell in the bristle lineage.

Fig. 1A-C illustrates a typical experiment intended to determine the period of the S-phase in the secondary precursor cells, pIIa and pIIb. The lineage was followed after the division of pI in several sensory organs (Fig. 1A). Results of this experiment are shown in Fig. 1B and data obtained from 27 pI cell divisions are compiled in Fig. 1C. After pI metaphase, the strongest homogeneous BrdU incorporation was always observed in pIIa and pIIb cells during the first 45 minutes (Fig. 1B, clusters 1 and 2). We were unable to visualise a G1-phase in these cells, even when dissection was performed earlier, during pI prophase. This suggests that the G1-phase, if present, is very short. One hour after pI metaphase and for a subsequent period of 15 minutes, punctuated BrdU incorporation was observed in both pIIa and pIIb cells (Fig. 1B cluster 3). This

punctuated immunoreactivity is reminiscent of the pattern of heterochromatin that is the last to be replicated (Foe et al., 1993), and as such we consider this pattern to mark the end of the S-phase. Later, around 1 hour after pI metaphase, there was no BrdU incorporation in either pIIa or pIIb precursor cells (Fig. 1B, cluster 4). These data indicate that the S-phase lasts for around 1 hour in both secondary precursor cells. As pIIb cells enter mitosis 30 minutes before pIIa, our data suggest that the G2-phase is longer in pIIa than in pIIb (1 hour 30 minutes for pIIa versus 1 hour for pIIb).

A similar protocol was applied to determine S-phase timing in the tertiary precursor cell, pIIIb (Fig. 1D-F). Results of this experiment are shown in Fig. 1E and data obtained from 26 pIIb cell divisions are compiled in Fig. 1F. After pIIb mitosis, there was a short period in which no BrdU incorporation was detected in the two progeny cells (glial and pIIIb cells) (Fig. 1E, cluster 1). Fifteen minutes after pIIb telophase, all pIIIb cells were BrdU-positive (Fig. 1E, clusters 2 and 3), indicating that in pIIIb the G1-phase is present, albeit of very short duration. The end of replication, revealed by spots of BrdU incorporation (Fig. 1E, cluster 4), was detected in pIIIb cells around 1 hour after pIIb metaphase. Thus, in pIIIb cells, the S-

phase lasts around 45 minutes. As this cell enters mitosis 2 hours after birth, the duration of the G2-phase is around 1 hour, similar to that observed in pIIb cells. During this entire period, we never observed BrdU incorporation in the glial cell, nor in the progeny of pIIa (socket and shaft cells).

Absence of G1-phase in the pIIa and pIIb precursor cells

The above-described experimental protocol does not allow one to detect a G1-phase shorter than 15 minutes, the time required for dissection and BrdU incubation. In order to reveal a possible G1-phase in the secondary precursor cells (pIIa and pIIb), we monitored the beginning of the S-phase by analysing BrdU incorporation directly during pI mitosis. To distinguish the pI cells and their descendants, we used the A101 strain that specifically expresses the *lacZ* gene in these cells (Usui and Kimura, 1993). Nota from A101 pupae at 17 hours APF, around the period of pI divisions, were dissected and incubated for 15 minutes in a BrdU-containing culture medium. Our data show that BrdU incorporation was already detectable in telophase cells. Telophase cells were identified by their small nuclei and the large space between them. To confirm these observations, triple staining was performed, labelling BrdU incorporation, nuclear envelope formation (by detection of lamin) (Newport and Forbes, 1987) and bristle lineage cells (by Sens immunoreactivity). Fig. 2A depicts a case in which both daughter nuclei are maximally separated; at this moment the nuclear envelope started to reform, as revealed by lamin immunodetection (note that a pool of lamin was still localized within the cytoplasm) and BrdU incorporation was already observed in both nuclei. The midbody, a bundle of microtubules at the point of cytokinesis, is another landmark of late telophase (Saxton and McIntosh, 1987). Triple staining was performed, labelling BrdU incorporation, midbody (using α-tubulin antibodies) and bristle lineage cells (by β-gal detection). Fig. 2B shows a typical case in which pIIa and pIIb incorporated BrdU at a moment in which a robust midbody was still present. Moreover, β-Gal, which is nuclear in the A101 strain, was still present in the cytoplasm when BrdU incorporation occurred. These data support the idea that the S-phase starts before the entire reformation of the nucleus. Taken together, these data suggest that the S-phase begins in late telophase of the pI division and that the G1-phase is absent in both secondary precursor cells, pIIb and pIIa.

A similar analysis was performed in pupae at 19 hours APF, during pIIb mitosis. In this case, BrdU was not incorporated during telophase, identified by the presence of a midbody (Fig. 2C), nor in interphase, just after formation of the nuclear envelope (Fig. 2D). No BrdU incorporation was observed in 22% of the three-cell sensory clusters analysed (*n*=28); these clusters contained young pIIIb cells, as pIIa had not yet divided. This low proportion of BrdU-negative three-cell clusters is consistent with our previous observations that the pIIIb cell cycle starts with a short G1-phase.

Endoreplication in pIIa progeny cells

Previous reports have shown that shaft and socket cells become polyploid by endoreplication (Hartenstein and Posakony, 1989). To determine the timing of DNA replication in these cells, nota from pupae between 21 and 36 hours APF were
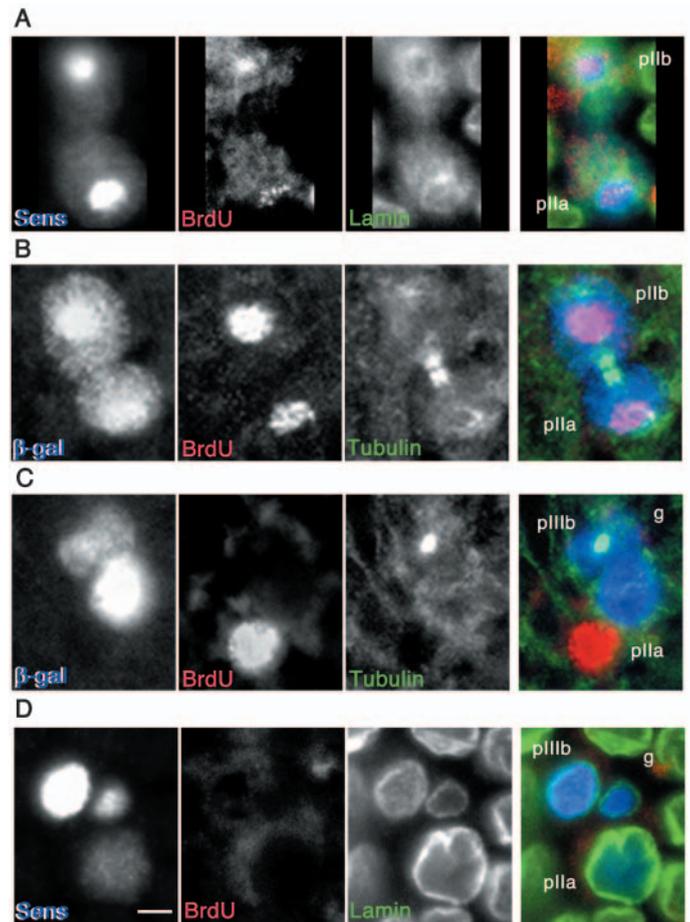
Fig. 2. S-phase entry in the secondary and tertiary precursor cells. BrdU incorporation (red) in A101 pupae at 17 hours APF during pI division (A-B) and in pupae at 19 hours APF during pIIb division (C-D). Bristle lineage cells were identified by specific anti-β-gal or anti-Sens immunoreactivity (blue). Cells in telophase were identified by incomplete formation of the nuclear envelope, as suggested by lamin immunoreactivity in the cytoplasm (A) and by the presence of the midbody (green) detected by α-Tub immunoreactivity (B,C). Note in C that that midbody is observed along the axis of division that follows an apico-basal orientation. In D, interphasic cells showing well-defined Lamin-labelling (green) around the nuclei. In each panel, overlay is on the right. Note in B that BrdU incorporation takes place in pIIa and pIIb cells, while the β-gal was still present in the cytoplasm. Note also that there is no BrdU incorporation late in pIIb telophase (C) and after formation of the pIIIb nucleus (D). Scale bar: 2 μm. g, glial cell.

incubated in a BrdU solution for a period of 1 or 2 hours and processed as previously described. The shaft and socket cells were identified by their size and their posterior position in the sensory clusters. In addition, socket cells were recognized by their specific accumulation of Su(H) (Gho et al., 1996). During the period studied, only the shaft and the socket cells incorporated BrdU. Four patterns of BrdU distribution were observed in sensory clusters: no BrdU incorporation (Fig. 3A), only the shaft cell positive for BrdU (Fig. 3B), only the socket cell positive for BrdU (Fig. 3C) and both cells BrdU-labelled (Fig. 3D). It is interesting to note that the socket cells underwent endoreplication when they were already engaged in

a specific pattern of cell fate determination as suggested by the Su(H) immunoreactivity.

The plot in Fig. 3E shows the percentage of clusters in which the shaft or socket cells incorporated BrdU. The data show that endoreplication occurred between 22 hours 30 minutes and 30 hours APF. Furthermore, the pattern of endoreplication for each cell appears bimodal, suggesting that the socket and the shaft cell undergo two successive rounds of DNA endoreplication: the shaft cell around 23 and 27 hours APF and the socket cell around 24 hours 30 minutes and 29 hours APF. The first phase of endoreplication overlaps in both cells, as revealed by clusters in which both cells were BrdU-positive (Fig. 3D; see also Fig. 7). The first observed BrdU-positive clusters (22 hours 30 minutes APF) have incorporated BrdU into the shaft cells (42%) or in both the shaft and the socket cells (58%). This suggests that these two cells do not enter the endoreplication phase simultaneously. Instead, the presence of clusters with BrdU-positive shaft cells only indicates that the shaft cells began DNA replication before the socket cells. After 30 hours APF, no BrdU incorporation was observed in the sensory clusters suggesting that the cells had become postmitotic. However, we did not extend our study beyond 36 hours APF and other rounds of replication could have occurred afterwards.

Expression pattern of Cyclin E and Dacapo proteins

Previous analyses have shown that CycE can be rate limiting for the progression from the G1- to S-phase (Knoblich et al., 1994). In order to determine whether the presence or absence of the G1-phase in cells of the bristle lineage is associated with a particular expression pattern of CycE, we analysed CycE immunoreactivity in fixed material. This analysis revealed a very dynamic expression pattern of CycE in cells of the bristle lineage. To accurately describe this expression pattern, these observations were complemented with experiments combining time-lapse imaging in living pupa followed by CycE detection (Fig. 4). CycE was detected in the pI precursor cell from 15 hours APF (Fig. 4A; see also Fig. 7) and it was inherited by the pIIa and pIIb daughter cells (Fig. 4B,C). Forty-five minutes after pIIa and pIIb formation, CycE was no longer detectable in these cells (Fig. 4D). Thirty minutes before mitosis, CycE

was detected again in pIIb (Fig. 4E). CycE was maintained for about 30 minutes in the pIIIb daughter cells while it disappeared faster in the glial cell (Fig. 4F,T). CycE protein was not detected in pIIIb for the next hour (not shown) and re-emerged 30 minutes before mitosis (Fig. 4G). After pIIIb division, CycE was inherited by the neuron and the sheath cell (Fig. 4H). Later, CycE rapidly vanished from these two cells. After 21 hours 30 minutes APF, CycE expression was no longer detected (Fig. 4I).

Our results show that the expression pattern of CycE was similar during the mitoses of pI, pIIb and pIIIb cells. However, a G1-phase follows the division of pIIb but not the division of pI. In order to identify factors that could account for this difference, we analysed the expression pattern of Dap, a Cdk2/CycE inhibitor (de Nooij et al., 1996). Initially (around 17 hours APF), Dap was absent in pI and its daughter cells, pIIa and pIIb (Fig. 4J,K). Dap was detected in pIIb before its division (Fig. 4L). This expression coincided with CycE (Fig. 4S). After the pIIb division, Dap was present in the two daughter cells (Fig. 4M). In the glial cell, Dap immunoreactivity persisted until its death by apoptosis (Fig. 4M-Q; note Dap-positive cell fragments in Q). By contrast, the initial expression observed in pIIIb vanished 15 minutes later (Fig. 4N,O). The loss of Dap preceded the decrement of CycE by at least 30 minutes. Thus in pIIIb, we observed high levels of CycE in the absence of its counterpart Dap (Fig. 4T). Dap reappeared in pIIIb before the cell divided (Fig. 4P) and was shutdown progressively in its progeny, the neuron and the sheath cell (Fig. 4Q). Finally, at around 25 hours APF, low levels of Dap were detected in the neuron as identified by ELAV expression (Fig. 4R). In pIIa, Dap was present before it divided (Fig. 4M,N) and was shutdown rapidly in its daughter cells: the socket and the shaft cells (Fig. 4O).

These results reveal some differences in the expression pattern of CycE and Dap (see Fig. 7). Firstly, during pI division, only CycE was present. Then, during pIIb and pIIIb divisions both factors were present. Interestingly, in pIIIb, which exhibits a G1-phase, Dap expression ceased when CycE was still strongly present. During pIIa division, Dap was present while CycE was no longer detected. Finally, we never detected Dap in late pIIa progeny cells.
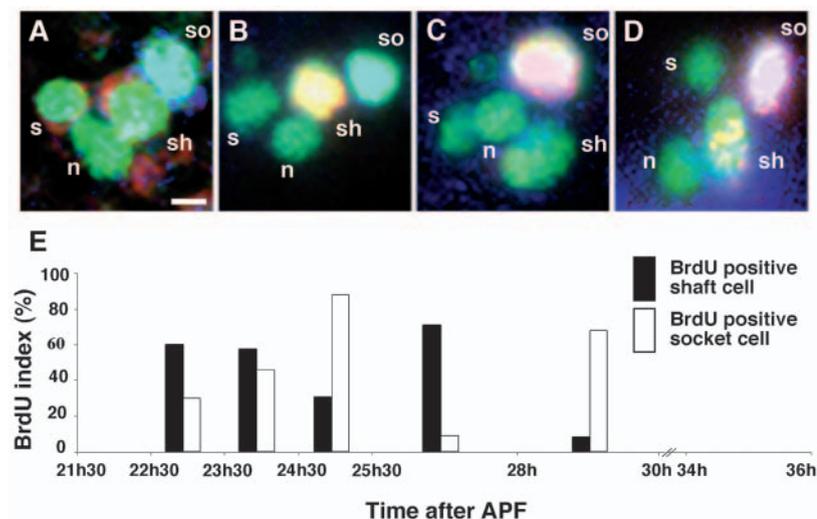
Fig. 3. Two rounds of endoreplication occurred in the socket and the shaft cells. Staining of nota from A101 pupae between 21 hours 30 minutes and 30 hours APF (A-D). β-Gal staining is in green, BrdU detection in red and Su(H) in blue. During this period, BrdU, when incorporated, was located in the shaft and/or the socket cells. Four types of clusters were observed: clusters with no BrdU labelling (A); clusters in which the shaft cell incorporated BrdU (B); clusters in which the socket cell incorporated BrdU (C); and clusters in which both the shaft and socket cells incorporated BrdU (D). (E) Histogram showing the percentage of clusters harbouring a BrdU-labelled shaft cell (black bars) or a BrdU-labelled socket cell (white bars) as a function of time after pupal formation. Note the bimodal distribution for each cell. Bars were calculated after analysis of 25 clusters. Scale bar: 2 μm. n, neuron; s, sheath cell; sh, shaft cell; so, socket cell.
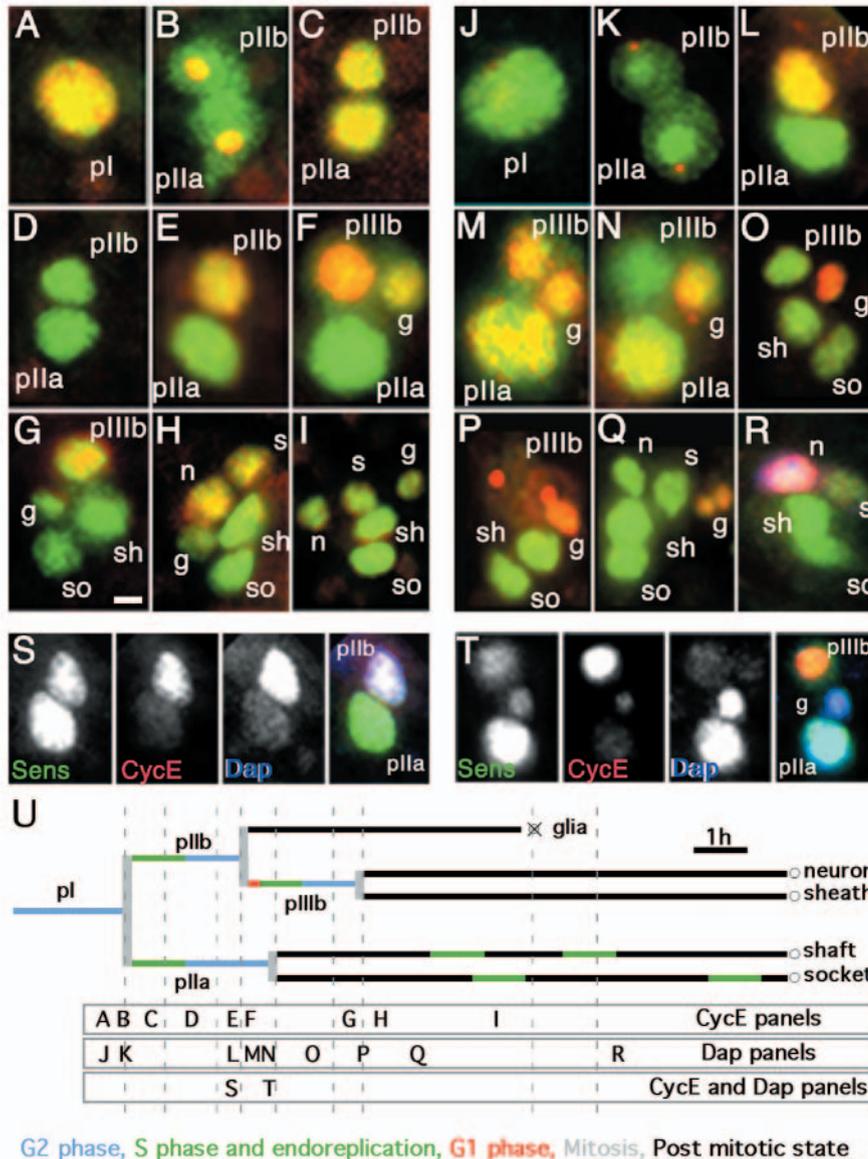
Fig. 4. Cyclin E and Dacapo expression pattern in the microchaete cell lineage. Staining of nota from A101 pupae between 16 and 24 hours APF. (A-I) CycE expression in bristle lineage cells at progressive stages of development. CycE staining is in red and β-gal staining in green. Combined time-lapse imaging of living pupae followed by CycE detection was performed in parallel to order the panel sequence. (J-R) Dap expression in bristle lineage cells at progressive stages of development. Dap staining is in red and β-gal staining in green. In R, the neuron is identified by Elav staining (blue). (S,T) Coexpression of CycE (red) and dap (blue) at a two (S) and three-cell (T) cluster stage as shown in E and L, in N and an intermediate stage between F and G, respectively. Sensory organ cells are stained by anti-Sens immunoreactivity (green). In S and T, the overlay is on the right. (U) Temporal localisation of each panel (A-T) during the cell lineage. Scale bar: 2 μm. g, glial cell, s, sheath cell; n, neuron; sh, shaft cell; so, socket cell.

The delayed entry into S-phase in pIIIb cells arises from Dap-inhibition of CycE/Cdk2 activity

In order to determine whether the differences in Dap and CycE expression can account for the acquisition of a G1-phase in the bristle lineage, we tested the possibility that the G1-phase arises in pIIIb due to the inhibition of the Cdk2/CycE complex by Dap. In an attempt to override the Dap-mediated inhibition, we analysed the G1-phase in pIIIb in a null *dap* background using the *dap⁴* strain (Hong et al., 2003) in which some homozygous escapers are viable until the pupal stage. Short duration BrdU incorporations were performed to analyse the BrdU incorporation pattern in three-cell clusters. This configuration ensures that the analysis was performed just after the pIIb division and before the pIIa division. Fig. 5A shows that BrdU incorporation took place during pIIb division when the midbody was still present. In the three-cell clusters analysed, 100% of the pIIIb cells and 93% of the glial cells were BrdU-labelled (*n*=56). These data show that, in *dap* null mutants, an S-phase can be induced late in telophase in the two

daughter cells arising from the pIIb division: a situation never observed in control animals.

Our observations suggest that the G1-phase in pIIIb cells results from the balance between CycE and Dap activities. Thus, in absence of Dap, S-phase is triggered in pIIIb cells just after their formation. To confirm this hypothesis, we overexpressed CycE to override Dap inhibition and we analysed the G1-phase in pIIIb in three-cell clusters. A high level of CycE accumulation in bristle lineage cells was obtained using the *neuᵖ⁷²*> CycE constructions. As before, BrdU incorporation was detected during the pIIb division at a time when the midbody was still present (Fig. 5B). This incorporation, when observed, occurred in the pIIIb cells. In 3% (compared with 22% in wild-type animals) of the three-cell clusters analysed, the pIIIb cell was not BrdU-labelled (*n*=36). These data indicate that under conditions of CycE overexpression the G1-phase in pIIIb is shorter than that in the control situation. In addition, at 20 hours APF, under conditions of CycE overexpression, BrdU incorporation was observed in
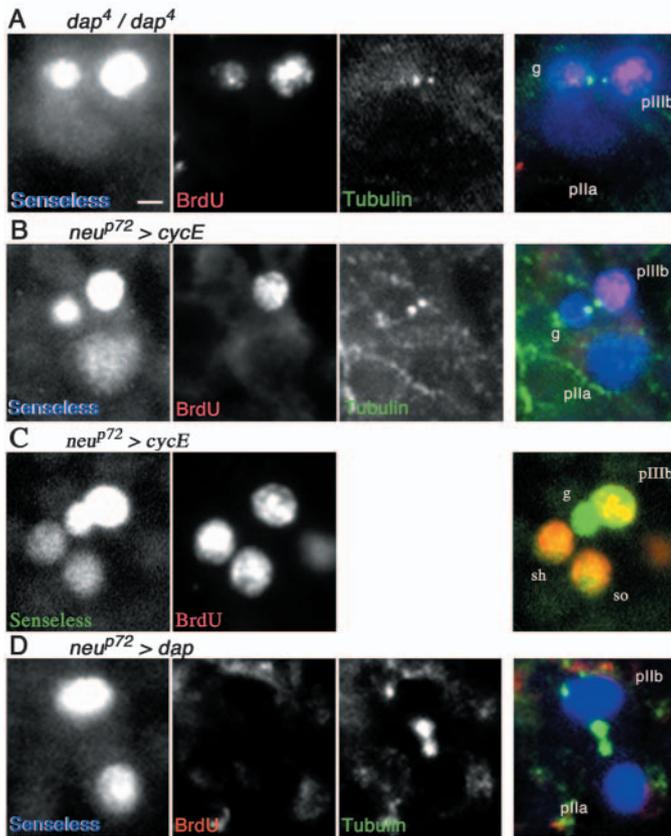
Fig. 5. The activity of CycE controls the G1 phase in secondary and tertiary precursor cells. (A) *dap⁴* null mutant pupae at 19 hours APF, BrdU incorporation (red) occurs during pIIb telophase, identified by the presence of the midbody (α-Tub, green). (B) After overexpression of CycE, BrdU incorporation (red) occurs during pIIb telophase, revealed by the midbody staining (α-Tub; green). Note that the BrdU-positive cell is the larger of the pair, suggesting that it corresponds to the pIIIb cell. Nota from *neu^P72^*> CycE pupae at 19 hours APF. (C) Overexpression of CycE induces precocious BrdU incorporation (red) in the shaft and the socket cells. Nota from *neu^P72^*> CycE pupae at 19 hours 30 minutes APF. Note that simultaneous BrdU incorporation in the pIIIb, the shaft and the socket cells was never observed in control animals.
(D) Overexpression of Dap triggered a G1-phase in pIIa and pIIb cells. By contrast to control animals (see Fig. 2A), no incorporation of BrdU (red) was observed during pI telophase, identified by the presence of the midbody (α-Tub; green). Nota from *neu^P72^*> Dap pupae around 17-18 hours APF. In all panels, sensory organ cells are identified by anti-Sens immunoreactivity (blue in A,B,D and green in C) and the overlay is on the right. g, glial cell; sh, shaft cell; so, socket cell. Scale bar: 2 μm.

the shaft and socket cells (80% of the four-cell cluster analysed) a situation never observed at this time in the wild-type flies (Fig. 5C). By contrast to the *dap⁴* homozygous experiments, no BrdU incorporation was detected in the glial cells when CycE was overexpressed. This suggests that Dap-inhibition is difficult to overcome. To further bypass this control, we overexpressed CycE in a genetic background heterozygous for *dap⁴*. Under these conditions, BrdU was incorporated in the glial cell in 35% of the three-cell clusters analysed (*n*=23). As before, 100% of pIIIb cells were BrdU-

positive. These data suggest that maintenance of Dap expression in the glial cell prevent the appearance of the S-phase. In addition, these observations confirm that the short presence of Dap in pIIIb cells induces a delayed entry into S-phase and the emergency of a G1-phase. Altogether our data show that, in control animals, the persistence of CycE triggered an S-phase in pIIIb cells only when the Dap-inhibition was overridden by the extinction of dap-expression.

High levels of CycE in the absence of Dap account for the absence of the G1-phase in secondary precursor cells

The Dap-dependent appearance of a G1-phase in the pIIIb cell suggests that the direct entry into the S-phase after pI division is due to the absence of this inhibitor. In order to test this hypothesis, we overexpressed Dap and determined whether or not an S-phase would occur during pI telophase as in the control situation. Experiments involving BrdU incorporation under conditions of Dap overexpression showed that at around 17 hours APF there was no DNA replication during pI telophase (Fig. 5D). This observation was confirmed in 100% of the late pI telophases analysed, a situation never observed in control conditions (see Fig. 2B). This absence of replication was correlated with an equal distribution of Dap immunoreactivity in both pI daughter cells. However, the S-phase was not abolished, as BrdU incorporation was observed in pIIa and pIIb cells at later stages (two-cell clusters without midbody) (not shown). Taken together, these results show that the balance of the activity between CycE/Cdk2 and Dap regulates the structure of the cell cycle in the bristle lineage cells. When CycE/Cdk2 overrides the inhibitory action of Dap, an S-phase is triggered (as is the case for pIIb, pIIa and in late pIIIb). However, when Dap controls the activity of this complex, no S-phase occurs and cells enter the G1-phase (as is the case for pIIIb) or become postmitotic (the terminal cells of the lineage).

CycE expression is controlled by Tramtrack p69

CycE protein was always re-expressed before pIIb and pIIIb mitosis but never before pIIa mitosis. We investigated whether a regulating factor ensured either the inhibition of *cycE* expression in pIIa cells and/or the induction of this expression in pIIb and pIIIb cells. In the embryonic nervous system, it has been shown that overexpression of the Ttk transcription factor blocks glial development by repressing expression of *cycE* (Badenhorst, 2001). As such we investigated the possibility that Ttk could prevent *cycE* expression in late pIIa cells and its descendants where CycE is not detected. In order to analyse this hypothesis, we studied the expression of Ttk in the bristle lineage. The *ttk* gene encodes two products, Ttk69 and Ttk88, via alternatively splicing (Read and Manley, 1992). An analysis of Ttk69 expression in bristle lineage cells revealed that this protein is expressed in the pIIa cell (Fig. 6A,B) and in its progeny, the shaft and the socket cells (Fig. 6C). After the pIIIb division, the sheath cell also becomes Ttk69 immuno-positive (Fig. 6C) (Lehembre et al., 2000). Thus, the expression pattern of Ttk in pIIa and its descendent is consistent with the possibility that Ttk prevents CycE expression in these cells. Previous clonal analysis, using the *ttk^osn^* allele, which affects both Ttk69 and Ttk88 proteins, revealed patches of adult cuticle devoid of outer support cells. In addition, sensory

organs were composed only of neurons, suggesting a transformation of pIIa into pIIb cells (Guo et al., 1995). This cell fate change prevents the analysis of CycE expression in a *ttk* null background. Thus, we analysed CycE expression in *ttk^{1e11}* somatic clones at 20 hours APF in which the Ttk69

Fig. 6. Ttk69 repressed CycE expression in pIIa cells.
(A-C) Expression pattern of Ttk in the bristle cell lineage. Ttk immunoreactivity (red) of nota from A101 pupae between 16 and 24 hours APF. Sensory organs were identified with anti β-gal antibodies (green). Note that Ttk expression preceded pIIa cell division. (D) Ttk overexpression repressed CycE expression in pIIb cells. A sensory organ from hs-Gal4>Ttk69 pupae. CycE detection is in red and Sens in green. Note that in three-cell clusters, CycE was not present in pIIIb cells (compare with control animals, Fig. 4F,T). (E-G) *ttk^{1e11}* somatic clones. Clones were detected by the lack of GFP staining (green), their limits are shown with a white dotted line. Sensory organs were detected with anti-Cut (E,F) and anti-Sens (G) antibodies (green). (E) Ttk69 protein is not detected in clusters in *ttk^{1e11}* somatic clones. Ttk protein is detected in red. Nota from pupae at 23 hours APF. (F) Socket cells are present in sensory organs inside *ttk^{1e11}* clones. Socket cells are identified by the high expression of Su(H) (red). Nota from pupae at 23 hours APF. In E and F, arrows indicate clusters located in the clone. (G) Ectopic CycE expression was observed in the progeny of pIIa cells in *ttk^{1e11}* somatic clones. Each panel is shown separately in G', G'', G'''. (G') *ttk^{1e11}* somatic clones identified by the lack of GFP staining, outlined by a white dotted line. Sensory organs were detected with anti-Sens antibodies. (G'') Prospero expression revealed the pIIb progeny (arrowheads). (G''') CycE accumulates in all cells of clusters inside the clone. Note that even pIIa daughter cells, identified by the lack of prospero staining (arrows), are CycE positive. Nota from pupae around 21 hours APF. g, glial cell; s, sheath cell; n, neuron; sh, shaft cell; so, socket cell. (A-D) Scale bars: 2 μm in A-D; 10 μm in E-G.
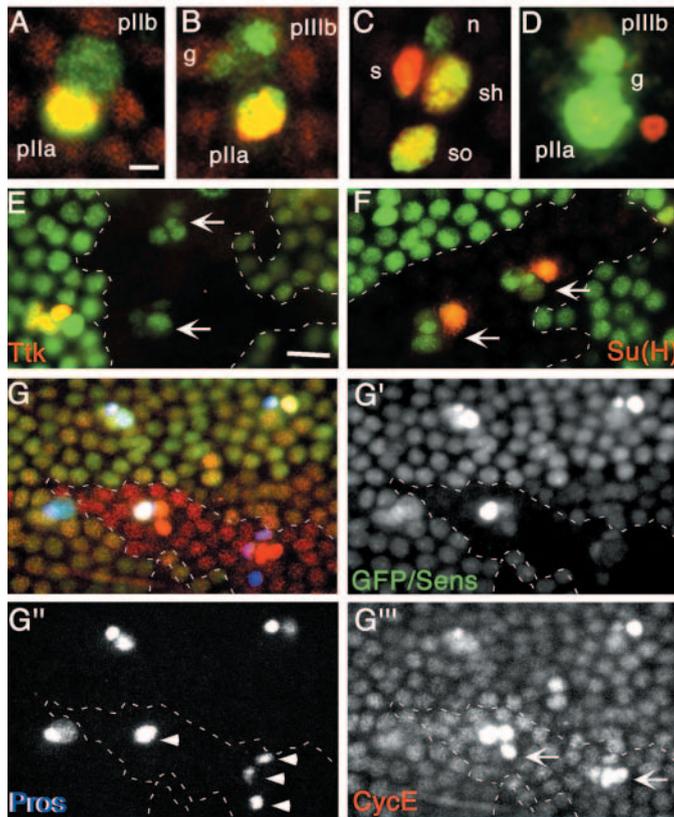
product is specifically depleted (Lai and Li, 1999). Accordingly, in *ttk^{1e11}* somatic clones, no Ttk69 was detected as revealed by the lack of immunoreactivity (Fig. 6E, arrows). In these clones, the existence of pIIa progeny in sensory organs was confirmed by the presence of both Prospero-negative cells (Fig. 6G'', arrowheads) (Gho et al., 1999) and Su(H)-positive socket cells (Fig. 6F, arrows) as well as socket cuticular structures in adult animals (not shown). These data show that Ttk69 is dispensable for the acquisition of pIIa fate and allow us to analyse, in a *ttk69* mutant background, the role of Ttk in CycE expression. We observed that inside *ttk^{1e11}* clones, all sensory cells expressed CycE. In particular, the two pIIa daughter cells, identified by the absence of Prospero immunoreactivity, strongly accumulated CycE, a situation never observed in non-clonal tissues (Fig. 6G-G''', arrows). Conversely, overexpression of the active form of Ttk69 prevented the expression of CycE. Thus, the expression of CycE in pIIIb, which was always observed in three-cell clusters, was abolished after overexpression of Ttk69 (Fig. 6D). Taken together these data indicate that Ttk regulates CycE expression in the bristle lineage. In particular, it prevents the expression of CycE in pIIa and its descendants. It is important to note that late in development (up to 24 hours APF), CycE was not detected in sensory organ cells inside the Ttk clone. This indicates that, in *ttk^{1e11}* clones, the CycE upregulation was transitory, suggesting that additional mechanisms acting late in development can be involved in the control of CycE expression.
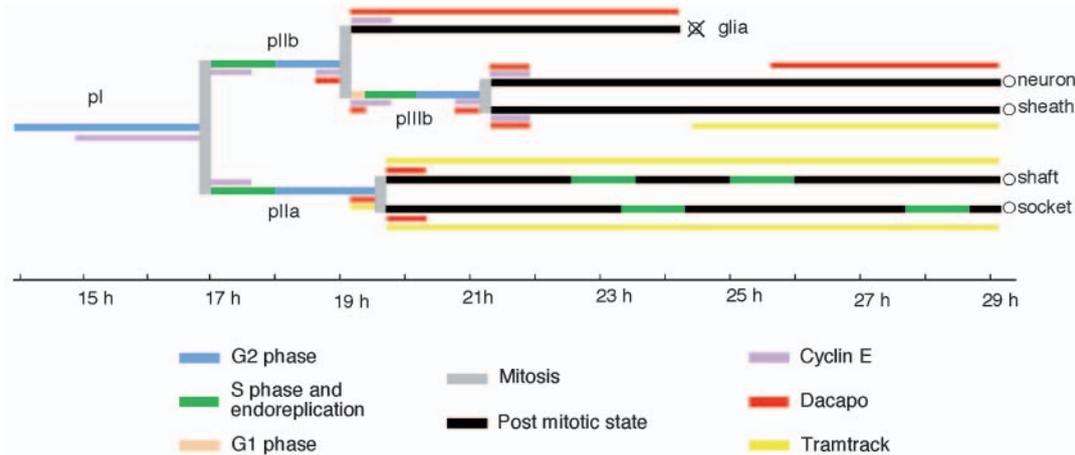
Discussion

The present study revealed that the cell cycle in bristle lineage cells was essentially modelled by the activity of CycE and its regulators Dap and Ttk. From direct observation of single precursor cells and BrdU-incorporation studies, we showed that this lineage harboured three cell cycle variants: (1) an atypical cell cycle, in which the G1-phase was missing, observed in the pIIa and pIIb cells; (2) a canonical cell cycle (S/G2/M/G1) with a short-lived G1-phase, which occurred in the pIIIb cell; and (3) endoreplicative cycles, where S-phases alternated with a gap phase without mitosis, observed in the socket and the shaft cells (Fig. 7). The two former variants were found in precursor cells, while the endoreplication occurred in differentiating cells.

Our data show that a similar expression of CycE, peaking during each mitosis, was observed in pI, pIIb and pIIIb cells, which exhibited atypical and canonical cell cycles. Moreover, Dap expression anticipated each mitosis, with the exception of the pI division, in which Dap was not observed. Thus, in the bristle lineage, Dap was expressed only during cell divisions giving rise to at least one postmitotic daughter cell. Therefore, one could hypothesise that Dap expression was controlled by a mechanism that counts cell divisions. In fact, this is not the case, as cell-cycle-arrested pI cells expressed Dap at later stages (Pierre Fichelson and M.G., unpublished). This observation suggests that Dacapo expression is controlled by a transcription factor with activity that changes progressively over time or by a cascade of sequentially activated factors acting independently of cell division.

We observed that neither the CycE nor the Dap proteins were detected in the shaft and socket cells during the period of

Fig. 7. Schematic representation of cell cycle phases and expression pattern of the CycE, Dap and Ttk proteins in the bristle cell lineage. The bristle lineage is represented by an arborisation where cell cycle phases are shown in different colours (see code). The length of each colour bar is proportional to the duration of each phase. The expression pattern of CycE, Dap and Ttk are represented by horizontal bars above or below the lineage branches. The cross over the glial cell indicates that this cell enters apoptosis. Time scale in hours APF.

endoreplication. This is unexpected, as it has been shown that one central regulator of Drosophila endocycles is the complex CycE/Cdk2 (Knoblich et al., 1994). However, in salivary glands and in ovary nurse cells, a downregulation of the CycE activity occurs to allow subsequent DNA replication (Sauer et al., 1995). During embryogenesis, progression through endoreplication requires the CycD/Cdk4 complex (Meyer et al., 2002a). Further analysis in our system, particularly concerning the function of the complex CycD/Cdk4, is necessary to reveal the mechanism underlying the cycles of endoreplications observed in the shaft and socket cells.

An atypical cell cycle without G1-phases in pIIa and pIIb

Several pieces of evidence indicate that the G1-phase is absent in secondary precursor cells and that these cells enter the S-phase directly. Thus, we observed pIIa and pIIb nuclei incorporate BrdU during late pI telophase, which was distinguishable by (1) presence of the midbody and (2) the cytoplasmic location of the nuclear envelope component lamin. That replication can occur before the end of mitosis has been observed in the embryonic cell cycle of *Xenopus*. In these cells, replication starts at early telophase. At this time, each chromosome becomes surrounded by a lamin-containing nuclear envelope, the karyomere (Lemaitre et al., 1998). This situation was never found during pI mitosis in the bristle lineage. Indeed, we observed that the nuclear envelope was formed around the entire chromosome set when we observed BrdU incorporation.

In *Drosophila*, the master cyclin/Cdk complex involved in the G1- to S-transition is the CycE/Cdk2 complex (Knoblich et al., 1994; Meyer et al., 2002a). Sustained expression of CycE has been observed during the rapid early divisions in *Drosophila* embryos. It is only after the destruction of the maternal stock and the zygotic activation of *string* and *cycE* genes that G2- and G1-phases appear in late embryos and larvae, respectively (Edgar and Lehner, 1996; Richardson et al., 1995). We observed that in the bristle lineage CycE expression preceded pI division. This expression was required for direct

transition to the S-phase after pI mitosis. Thus, the S-phase was delayed after a reduction in the CycE activity produced by Dap overexpression. Therefore, sustained expression of CycE before and after mitosis ensures the direct transition from M- to S-phases in both the early embryo and the bristle cell lineage.

High levels of CycE are necessary but not sufficient to trigger the S-phase. For example, pI cells, which are arrested in G2 (Kimura et al., 1997), express CycE around 2 hours before division. However, these cells do not enter the S-phase. Similar observations have been made in amnioserosa cells and non-proliferating pole cells (Richardson et al., 1993; Su et al., 1998). This refractory property is certainly due to the mechanism that prevents DNA replication during G2-arrested cells. This mechanism exerts a control over the licensing factors through mitotic Cdk/cyclin complexes rather than inactivating the CycE activity (Sauer et al., 1995).

A dispensable G1-phase in pIIIb

CycE expression anticipates pIIb division, which confers to its progeny (the pIIIb and the glial cell) the capacity to precociously enter the S-phase, as is the case for secondary precursor cells resulting from the pI division. However, both pIIb descendents express Dap and do not enter the S-phase. Our data suggest that Dap expression downregulates CycE activity in glial cells, which rapidly enter a postmitotic state. Dap expression is required to trigger a postmitotic state, as S-phases can be induced in glial cells in a *dap* null mutant homozygous background. Furthermore, glial cell division was occasionally observed after CycE overexpression in a *dap* mutant background (A.A., F.S. and Pierre Fichelson, unpublished). We think that the ephemeral G1-phase present in pIIIb is due to the fortuitous inheritance of Dap, which triggers a postmitotic state in its sister cell, the glia. No change in pIIIb fate was observed after reduction of the G1 duration, indicating that the G1-phase is dispensable for the identity of this cell. Thus, the G1-phase in pIIIb seems to be a secondary effect of the glial cell commitment to a postmitotic state. Taken together, our results suggest that, in non-terminal cells, the

expression of CycE late in the G2-phase leads to the next cell cycle essentially devoid of G1-phase.

Tramtrack-69 downregulates Cyclin E activity

The *ttk* gene encodes two alternatively spliced zinc-finger transcription factors, Ttk69 and Ttk88 (Read and Manley, 1992). Previous analyses have shown that Ttk products act downstream of Notch and are involved in the control of non-neural cell fates (Guo et al., 1995). The persistent expression of Ttk69 in the socket, shaft and late sheath cells is coherent with this function. Surprisingly, our clonal analysis using the *ttk^{1e11}* allele, which affects specifically Ttk69 (Lai and Li, 1999), showed that socket cells and neurons are found in sensory organs inside *ttk* clones. These results suggested that Ttk69 is dispensable for acquisition of socket identity. Clonal analysis using *ttk* alleles affecting specifically Ttk88 will be required to determine whether this form is necessary or only sufficient to determine a socket fate.

In the embryonic central nervous system, it has been proposed that Ttk69, apart from its role as a determinant, controls cell proliferation. This control seems to involve the repression of *cycE* and *string* gene expression (Badenhorst, 2001; Baonza et al., 2002). We took advantage of the fact that the pIIa fate was not abolished in *ttk^{1e11}* to analyse the role of Ttk in *cycE* expression. We have shown that, in a *ttk^{1e11}* mutant background where Ttk69 is lost, pIIa daughter cells ectopically expressed CycE. Conversely, overexpression of Ttk69 resulted in a loss of *cycE* expression in pIIb cells. These results show that the Ttk expression in pIIa and its daughter cells prevents expression of CycE. The effect of Ttk69 on CycE was transitory, and CycE accumulation in pIIa progeny cells was not observed in *ttk^{1e11}* clones at 24 hours APF. Although CycE ectopic expression was transitory, we have observed supplementary cell divisions in sensory organs inside *ttk^{1e11}* clones. Accordingly, 80% of clonal sensory organs were composed of five to six cells, compared with only four in control clusters (data not shown). The transitory ectopic expression of CycE suggests that Ttk69 is responsible only in part for downregulation of *cycE* in pIIa progeny. Thus, additional mechanisms must also be involved in the control of CycE expression. In particular, one possibility is that Ttk88 can compensate for the lack of Ttk69. Unfortunately, the role of Ttk in determining cell fate identity prevents us from analysing CycE expression in a completely null *ttk* background. In any case, our results suggest that, in the bristle lineage, apart from its role in establishing cell fate identity, Ttk is involved in the cell cycle exit, and/or maintenance of a postmitotic state, via the downregulation of CycE.

Atypical cell cycles and asymmetric cell divisions assure a rapid cadence of cell divisions in the bristle lineage

The period between each division in the bristle lineage is around 2.5 hours. This high rate of cell division suggests that in this lineage cell size is not a limiting factor for cell cycle progression. At each division, Notch-mediated cell decisions are biased by the presence in one daughter cell of Numb and Neuralized that assure the activation of the Notch pathway in the other daughter cell (Jan and Jan, 1998; Le Borgne and Schweisguth, 2003). Thus, the asymmetric nature of cell divisions in the bristle lineage could shortening the amount of

time required for the activation of the Notch pathway in one daughter cell. In addition, previous analysis of the Notch-mediated cell decisions during vulva formation of *Caenorhabditis elegans* (Ambros, 1999) suggests that the Notch response can be implemented during the S-/G2-phase. Therefore, it is expected that the reduction, or even the elimination, of the G1-phase does not have an impact on the Notch-mediated cell fate decisions. Taken together, these data suggest that the asymmetry in cell divisions and the absence of the G1-phase can be seen as mechanisms that have been introduced into stochastic cell lineages during evolution, thus allowing a very rapid succession of cell divisions.

References

Ambros, V. (1999). Cell cycle-dependent sequencing of cell fate decisions in Caenorhabditis elegans vulva precursor cells. *Development* **126**, 1947-1956.

Badenhorst, P. (2001). Tramtrack controls glial number and identity in the *Drosophila* embryonic CNS. *Development* **128**, 4093-4101.

Baonza, A., Murawsky, C. M., Travers, A. and Freeman, M. R. (2002). Pointed and Tramtrack69 establish an EGFR-dependent transcriptional switch to regulate mitosis. *Nat. Cell Biol.* **4**, 976-980.

Bellaiche, Y., Gho, M., Kaltschmidt, J. A., Brand, A. H. and Schweisguth, F. (2001). Frizzled regulates localization of cell-fate determinants and mitotic spindle rotation during asymmetric cell division. *Nat. Cell Biol.* **3**, 50-57.

Brand, A. H. and Perrimon, N. (1993). Targeted gene expression as a means of altering cell fates and generating dominant phenotypes. *Development* **118**, 401-415.

de Nooij, J. C., Letendre, M. A. and Hariharan, I. K. (1996). A cyclin-dependent kinase inhibitor, Dacapo, is necessary for timely exit from the cell cycle during *Drosophila* embryogenesis. *Cell* **87**, 1237-1247.

Edgar, B. A. and Lehner, C. F. (1996). Developmental control of cell cycle regulators: a fly's perspective. *Science* **274**, 1646-1652.

Edgar, B. A. and Orr-Weaver, T. L. (2001). Endoreplication cell cycles: more for less. *Cell* **105**, 297-306.

Fichelson, P. and Gho, M. (2003). The glial cell undergoes apoptosis in the microchaete lineage of *Drosophila*. *Development* **130**, 123-133.

Foe, V. E., Odell, G. M. and Edgar, B. A. (1993). Mitoses and morphogenesis in the Drosophila embryo: point and counterpoint. In *The Development of Drosophila melanogaster* (ed. M. Bate and A. Martinez Arias), pp. 149-300. Cold Spring Harbor, NY: Cold Spring Harbor Laboratory Press.

Gho, M., Lecourtois, M., Geraud, G., Posakony, J. W. and Schweisguth, F. (1996). Subcellular localization of Suppressor of Hairless in *Drosophila* sense organ cells during Notch signalling. *Development* **122**, 1673-1682.

Gho, M., Bellaiche, Y. and Schweisguth, F. (1999). Revisiting the *Drosophila* microchaete lineage: a novel intrinsically asymmetric cell division generates a glial cell. *Development* **126**, 3573-3584.

Guo, M., Bier, E., Jan, L. Y. and Jan, Y. N. (1995). tramtrack acts downstream of numb to specify distinct daughter cell fates during asymmetric cell divisions in the *Drosophila* PNS. *Neuron* **14**, 913-925.

Hartenstein, V. and Posakony, J. W. (1989). Development of adult sensilla on the wing and notum of *Drosophila* melanogaster. *Development* **107**, 389-405.

Hong, A., Lee-Kong, S., Iida, T., Sugimura, I. and Lilly, M. A. (2003). The p27cip/kip ortholog dacapo maintains the *Drosophila* oocyte in prophase of meiosis I. *Development* **130**, 1235-1242.

Jan, Y. N. and Jan, L. Y. (1998). Asymmetric cell division. *Nature* **392**, 775-778.

Kimura, K., Usui-Ishihara, A. and Usui, A. (1997). G2 arrest of cell cycle ensures a determination process of sensory mother cell formation in *Drosophila*. *Dev. Genes Evol.* **207**, 199-202.

Knoblich, J. A., Sauer, K., Jones, L., Richardson, H., Saint, R. and Lehner, C. F. (1994). Cyclin E controls S phase progression and its down-regulation during *Drosophila* embryogenesis is required for the arrest of cell proliferation. *Cell* **77**, 107-120.

Lai, Z. C. and Li, Y. (1999). Tramtrack69 is positively and autonomously required for *Drosophila* photoreceptor development. *Genetics* **152**, 299-305.

Lane, M. E., Sauer, K., Wallace, K., Jan, Y. N., Lehner, C. F. and Vaessin, H. (1996). Dacapo, a cyclin-dependent kinase inhibitor, stops cell proliferation during *Drosophila* development. *Cell* **87**, 1225-1235.

Le Borgne, R. and Schweisguth, F. (2003). Unequal segregation of Neuralized biases Notch activation during asymmetric cell division. *Dev. Cell* **5**, 139-148.

Lehembre, F., Badenhorst, P., Muller, S., Travers, A., Schweisguth, F. and Dejean, A. (2000). Covalent modification of the transcriptional repressor tramtrack by the ubiquitin-related protein Smt3 in *Drosophila* flies. *Mol. Cell Biol.* **20**, 1072-1082.

Lemaitre, J. M., Geraud, G. and Mechali, M. (1998). Dynamics of the genome during early *Xenopus Laevis* development: karyomeres as independent units of replication. *J. Cell Biol.* **142**, 1159-1166.

Malumbres, M., Sotillo, R., Santamaria, D., Galan, J., Cerezo, A., Ortega, S., Dubus, P. and Barbacid, M. (2004). Mammalian cells cycle without the D-type cyclin-dependent kinases Cdk4 and Cdk6. *Cell* **118**, 493-504.

Meyer, C. A., Jacobs, H. W. and Lehner, C. F. (2002a). Cyclin D-cdk4 is not a master regulator of cell multiplication in *Drosophila* embryos. *Curr. Biol.* **12**, 661-666.

Meyer, C. A., Kramer, I., Dittrich, R., Marzodko, S., Emmerich, J. and Lehner, C. F. (2002b). *Drosophila* p27Dacapo expression during embryogenesis is controlled by a complex regulatory region independent of cell cycle progression. *Development* **129**, 319-328.

Newport, J. W. and Forbes, D. J. (1987). The nucleus: structure, function, and dynamics. *Annu. Rev. Biochem.* **56**, 535-565.

Nolo, R., Abbott, L. A. and Bellen, H. J. (2000). Senseless, a Zn finger transcription factor, is necessary and sufficient for sensory organ development in *Drosophila*. *Cell* **102**, 349-362.

Read, D. and Manley, J. L. (1992). Alternatively spliced transcripts of the *Drosophila* tramtrack gene encode zinc finger proteins with distinct DNA binding specificities. *EMBO J.* **11**, 1035-1044.

Richardson, H., O'Keefe, L. V., Reed, S. I. and Saint, R. (1993). A *Drosophila* G1-specific cyclin E homolg exhibits different modes of expression during embryogenesis. *Development* **119**, 673-690.

Richardson, H., O'Keefe, L. V., Marty, T. and Saint, R. (1995). Ectopic cyclin E expression induces premature entry into S phase and disrupts pattern formation in the *Drosophila* eye imaginal disc. *Development* **121**, 3371-3379.

Sauer, K., Knoblich, J. A., Richardson, H. and Lehner, C. F. (1995). Distinct modes of cyclin E/cdc2c kinase regulation and S-phase control in mitotic and endoreduplication cycles of *Drosophila* embryogenesis. *Genes Dev.* **9**, 1327-1339.

Saxton, W. M. and McIntosh, J. R. (1987). Interzone microtubule behavior in late anaphase and telophase spindles. *J. Cell Biol.* **105**, 875-886.

Su, T. T., Campbell, S. D. and O'Farrell, P. H. (1998). The cell cycle program in germ cells of *Drosophila* embryo. *Dev. Biol.* **196**, 160-170.

Usui, K. and Kimura, K. I. (1993). Sequential emergence of the evenly spaced microchaetes on the notum of *Drosophila*. *Roux's Arch. Develop. Biol.* **203**, 151-158.

Vidwans, S. J. and Su, T. T. (2001). Cycling through development in *Drosophila* and other metazoa. *Nat. Cell Biol.* **3**, E35-E39.

Development